BNL-73312-2004-JA-R1

GEOPHYSICAL RESEARCH LETTERS, VOL. 32, L05708, doi:10.1029/2004GL021922, 2005

A smaller global estimate of the second indirect aerosol effect

Leon D. Rotstayn

Atmospheric Research, Commonwealth Scientific and Industrial Research Organisation, Aspendale, Victoria, Australia

Yangang Liu

Atmospheric Sciences Division, Brookhaven National Laboratory, Upton, New York, USA

Received 5 November 2004; revised 20 December 2004; accepted 7 February 2005; published 8 March 2005.

[1] Global estimates of the indirect aerosol effect much larger than 1 W m^{-2} in magnitude are difficult to reconcile with observations, yet climate models give estimates between -1 and -4.4 W m^{-2}. We use a climate model with a new treatment of autoconversion to reevaluate the second indirect aerosol effect. We obtain a global-mean value of -0.28 W m^{-2}, compared to -0.71 W m^{-2} with the autoconversion treatment most often used in climate models. The difference is due to (1) the new scheme's smaller autoconversion rate, and (2) an autoconversion threshold that increases more slowly with cloud droplet concentration. The impact of the smaller autoconversion rate shows the importance of accurately modeling this process. Our estimate of the total indirect aerosol effect on liquid-water clouds changes from -1.63 to -1.09 W m^{-2}.

Citation: Rotstayn, L. D., and Y. Liu (2005), A smaller global estimate of the second indirect aerosol effect, *Geophys. Res. Lett.*, *32*, L05708, doi:10.1029/2004GL021922.

1. Introduction

[2] The most uncertain of the anthropogenic climate forcings are the indirect aerosol effects on clouds. Estimates for the first indirect effect, whereby an increase in aerosols leads to a decrease in cloud-droplet effective radius and hence an increase in cloud albedo, range from 0 to -2 W m^{-2} according to *Intergovernmental Panel on Climate Change* (*IPCC*) [2001a, 2001b]. The second indirect aerosol effect, whereby smaller droplets in polluted clouds form raindrops less efficiently, was considered too uncertain to be included in the IPCC's estimates. Simulations using global climate models (GCMs) suggest that the second indirect effect should enhance the first indirect effect, by increasing cloud liquid-water path [*IPCC*, 2001b]. Estimates in the range of -1 to -4.4 W m^{-2} for the combined indirect effect have been obtained in recent GCMs [*Ghan et al.*, 2001; *Jones et al.*, 2001; *Lohmann and Feichter*, 2001; *Kristjánsson*, 2002; *Menon et al.*, 2002; *Suzuki et al.*, 2004]. However, such large estimates are difficult to reconcile with observed temperature records [*Anderson et al.*, 2003]. Furthermore, a general increase of cloud liquid-water path with increased aerosol loading, as predicted by GCM simulations, has not been found in recent empirical studies [e.g., *Han et al.*, 2002].

[3] These discrepancies between GCMs and observations suggest that indirect aerosol effects may be overestimated in GCMs [*Lohmann and Lesins*, 2002]. A partial explanation was offered by *Liu and Daum* [2002], who showed that increases in cloud droplet concentration are associated with increased dispersion (breadth) of the cloud droplet size distribution, and that the increased dispersion counteracts the first indirect aerosol effect. Subsequent GCM simulations have confirmed that neglect of the dispersion effect can lead to overestimation of the first indirect aerosol effect [*Peng and Lohmann*, 2003; *Rotstayn and Liu*, 2003].

[4] It is also expected from cloud physics theory [*Beard and Ochs*, 1993] that increased dispersion will enhance the coalescence of cloud droplets (autoconversion) and thereby offset the second indirect effect, but this has been ignored in GCMs. In this paper, we present new GCM-based calculations of the second indirect effect using a new autoconversion scheme, which accounts for the dispersion effect. We also recalculate the second indirect effect using the autoconversion scheme that has been most widely used in GCMs, and explain the reasons for the smaller result obtained with the new scheme.

2. Autoconversion Parameterizations

[5] The autoconversion parameterization ("R_3 scheme") most widely used in GCM simulations of the second indirect effect [*Rotstayn*, 2000; *Ghan et al.*, 2001; *Jones et al.*, 2001; *Kristjánsson*, 2002; *Menon et al.*, 2002] can be expressed as [*Baker*, 1993; *Boucher et al.*, 1995]

$$P = E_c \pi \kappa_1 \left(\frac{3}{4\pi\rho_l}\right)^{4/3} N^{-1/3} L^{7/3} H(R_3 - R_{3c}), \qquad (1)$$

where P is the rate of decrease of liquid-water content due to autoconversion, E_c is a constant collection efficiency, $\kappa_1 = 1.19 \times 10^6$ cm^{-1}s^{-1} is the Stokes constant, ρ_l is the density of liquid water, N is the droplet number concentration, L is the liquid-water content, R_{3c} is a prescribed critical droplet radius, and R_3 is the volume-weighted mean radius. (R_p is the mean radius of the pth moment of the droplet-size distribution, defined by $R_p = (\int R^p n(R) dR/N)^{1/p}$, where $n(R)dR$ is the number concentration of droplets with radii between R and $R + dR$.) The Heaviside function $H(R_3 - R_{3c})$ suppresses autoconversion unless R_3 exceeds R_{3c}. The critical radius is usually "tuned" in GCMs to obtain a realistic simulation; values between 4.5 and 10 μm have been adopted. E_c is typically assumed to equal 0.55, but several authors have argued that this value is much too large [*Baker*, 1993; *Austin et al.*, 1995; *Khairoutdinov and Kogan*, 2000].

[6] However, this scheme does not account for the dispersion effect, and also employs the unrealistic assump-

0094-8276/05/2004GL021922$05.00

tion of constant collection efficiency. A new autoconversion parameterization ("R_6 scheme"), which removes these limitations, is [*Liu and Daum*, 2004; *Liu et al.*, 2004]

$$P = \left(\frac{3}{4\pi\rho_l}\right)^2 \frac{\kappa_2 \beta_6^6}{N} L^3 H(R_6 - R_{6c}), \tag{2}$$

where R_6 is the mean radius of the sixth moment of the droplet size distribution, and $\kappa_2 = 1.9 \times 10^{11}$ cm^{3}s^{-1} is a constant from the Long collection kernel, which represents the increase of collection efficiency with increasing collector drop size. The dispersion effect is described by $\beta_6 = R_6/R_3$, where, assuming a gamma distribution for the cloud-droplet spectrum,

$$\beta_6 = \left[\frac{(1+3\epsilon^2)(1+4\epsilon^2)(1+5\epsilon^2)}{(1+\epsilon^2)(1+2\epsilon^2)},\right]^{1/6}, \tag{3}$$

where ϵ is the relative dispersion of the droplet size distribution (ratio of the standard deviation to the mean radius). Instead of using a fixed critical radius, R_{6c} was derived as a function of L and N by *Liu et al.* [2004] as

$$R_{6c} = 4.09 \times 10^{-4} \beta_{\rm con}^{1/6} \frac{N^{1/6}}{L^{1/3}}, \tag{4}$$

where R_{6c} is in μm, L in g m^{-3}, N in cm^{-3} and $\beta_{\rm con} = 1.15 \times 10^{23}$ s^{-1} is the mean value of the condensation rate constant. Due to scatter in the measurements, there is considerable uncertainty in $\beta_{\rm con}$, and hence in R_{6c}. A parameterization for the relative dispersion is [*Rotstayn and Liu*, 2003]

$$\epsilon = 1 - 0.7\exp(-\alpha N), \tag{5}$$

where $\alpha = 0.003$ gave a good fit to the data, although the presence of considerable scatter was noted.

[7] In a GCM, the critical droplet radius is used to calculate L_c, the critical liquid-water content for the onset of autoconversion. In the R_3 scheme, L_c is trivially obtained as

$$L_c = \frac{4\pi\rho_l}{3} R_{3c}^3 N. \tag{6}$$

When using the R_6 scheme, R_{6c} is parameterized using equation (4). Then, use of $R_{3c} = R_{6c}/\beta_6$ and equation (6) gives

$$L_c = \frac{4\pi\rho_l}{3L}\left(\frac{4.09 \times 10^{-4}\beta_{\rm con}^{1/6} N^{1/2}}{\beta_6}\right)^3. \tag{7}$$

At the critical point, $L = L_c$, so a unique expression for L_c in terms of N can be obtained by setting $L = L_c$ in equation (7) and solving for L_c.

3. Model and Experiments

[8] To quantify the impact of the R_6 scheme on the second indirect effect, we used the CSIRO Mark3 GCM [*Gordon et al.*, 2002] at low resolution (spectral R21). The model has been updated by treatments of the tropospheric sulfur cycle [*Rotstayn and Lohmann*, 2002] and carbonaceous aerosols (based on *Cooke and Wilson* [1996]). Sea-salt aerosol in the marine boundary layer is diagnosed as a function of windspeed [*O'Dowd et al.*, 1997]. The present-day (PD) emissions are applicable to the 1980s, and follow *Rotstayn and Lohmann* [2002] for the sulfur emissions, and *IPCC* [2001b] for the carbonaceous aerosols. Preindustrial (PI) emissions are obtained by setting the industrial emissions to zero, and the biomass-burning emissions to 10% of the PD values.

Table 1. Global-Mean Cloud Liquid-Water Path (LWP) and Top-of-Atmosphere Shortwave Cloud Forcing (SCF) From Each Simulation, and the Difference in Net Cloud Radiative Forcing (ΔCF) Between the PD and PI Simulations of Each Pair[a]

	R3AUTO		R6C_R3RATE		R6AUTO	
	PD	PI	PD	PI	PD	PI
LWP	58.02	55.01	57.86	55.47	63.56	62.14
SCF	−49.22	−48.39	−49.25	−48.63	−50.88	−50.56
ΔCF	−0.71		−0.52		−0.28	

[a]LWP in g m^{-2}; SCF and ΔCF in W m^{-2}.

[9] The model includes a detailed cloud microphysical scheme [*Rotstayn*, 1997; *Rotstayn and Liu*, 2003]. N as used to calculate autoconversion is estimated empirically from the mass concentrations of sulfate, organic matter and sea-salt aerosol [*Menon et al.*, 2002]. A minimum value of N = 20 cm^{-3} is applied, and there are no effects of aerosols on convective clouds or ice clouds.

[10] We performed three (PD and PI) pairs of simulations, to identify the effect of using the R_6 scheme (equations (2) and (7)) instead of the R_3 scheme (equations (1) and (6)):

[11] 1. R3AUTO: Autoconversion is calculated using the R_3 scheme for the autoconversion rate and threshold, with R_{3c} = 7.5 μm.

[12] 2. R6C_R3RATE: The autoconversion rate follows the R_3 scheme, but the threshold follows the R_6 scheme.

[13] 3. R6AUTO: Both the autoconversion rate and threshold follow the R_6 scheme.

[14] To suppress the first indirect effect, N as used to calculate the droplet effective radius in the radiation scheme was prescribed as 300 cm^{-3} over land and 100 cm^{-3} over oceans. No direct aerosol effects were allowed, and the concentration of CO_2 was held fixed at 345 ppm. We ran the model for 21 years with prescribed, monthly mean sea-surface temperatures. The first year of each simulation was discarded as a "spinup" period, and statistics were obtained from the remaining 20 years.

4. Results and Discussion

[15] Table 1 summarizes the results from the three pairs of simulations. First, note that the R_6 scheme gives reasonable global-mean values of shortwave cloud forcing (SCF) and liquid-water path (LWP) without any retuning of the model. This needs further investigation, since we did not explicitly consider the effects of subgrid variability in cloud-water content [e.g., *Rotstayn*, 2000]. The difference in net cloud forcing (ΔCF) between the PD and PI runs gives an estimate of the second indirect aerosol effect, including the small longwave component. The second indirect effect is about 61% smaller in the R6AUTO runs (−0.28 W m^{-2}) com-

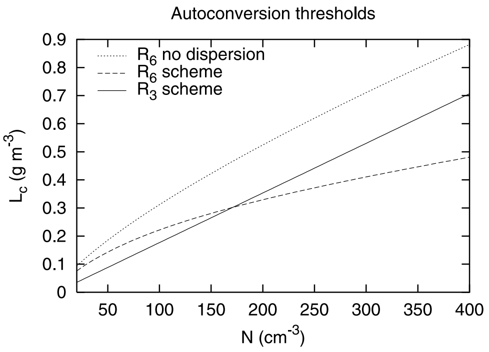

Figure 1. Autoconversion thresholds given by the R_3 scheme with R_{3c} = 7.5 μm, and by the R_6 scheme with and without the dispersion effect. See color version of this figure in the HTML.

pared to the R3AUTO runs (−0.71 W m^{-2}). The value from the R6C_R3RATE run lies in between the other two, showing that the R_6 schemes for the autoconversion rate and threshold both act to reduce the second indirect effect in our model. For each pair of simulations, the difference in LWP is qualitatively consistent with the difference in SCF.

[16] To explain why the R_6 threshold gives a smaller second indirect effect than the R_3 threshold, Figure 1 shows L_c versus N for the R_3 scheme (equation (6)) and the R_6 scheme (equation (7)). Without the dispersion effect (β_6 = 1), the R_6 scheme gives a stronger increase of L_c with N than the R_3 scheme, because R_{6c} increases with N (equation (4)) instead of being fixed. Inclusion of the dispersion effect in the R_6 scheme (equations (3) and (5)) reduces the slope of the L_c versus N curve. Compared to the R_3 scheme, the R_6 scheme with dispersion gives larger L_c for small N and smaller L_c for large N, and thus gives a smaller second indirect effect.

[17] To understand why the R_6 rate gives a smaller second indirect effect than the R_3 rate, we plot the autoconversion rates versus N for L = 0.3 g m^{-3} in Figure 2. Figure 2a uses a logarithmic scale for the vertical axis, so that the slope ($d$log P/dN) shows the relative changes of P. The autoconversion rate is smaller in the R_6 scheme than in the R_3 scheme (and even more so without the dispersion effect). This explains why R6AUTO has larger values of LWP than R6C_R3RATE. Without the dispersion effect, the steeper decrease of P with N in the R_6 scheme (N^{-1}) compared to the R_3 scheme ($N^{-1/3}$) is evident. Inclusion of the dispersion effect in the R_6 scheme brings the slope of the P versus N curve closer to that of the R_3 scheme, though it is still steeper for small values of N.

[18] However, an important point is that the magnitude of the second indirect effect depends on absolute changes of P with N, as shown by the slopes of the curves in Figure 2b, which uses a linear scale. Inclusion of the dispersion effect in the R_6 scheme markedly increases P, but only slightly increases the decrease of P with N. Since P is much smaller in the R_6 scheme than in the R_3 scheme, the decrease of P with N is also smaller. (If $P \propto N^{-\gamma}$, then $dP/dN = -\gamma PN^{-1}$, where γ = 1/3 in the R_3 scheme and γ = 1 in the R_6 scheme without the dispersion effect. Figure 2b shows that, without the dispersion effect, P is more than 3 times smaller in the R_6 scheme than in the R_3 scheme, so dP/dN is also smaller. The dispersion effect modifies the above by increasing P and decreasing the effective value of γ. The net dispersion effect depends on the competition between these two effects; the slopes of the two lower curves in Figure 2b show that they roughly balance for large N, and the effect of increased P is stronger for small N.)

[19] Previous indications that the autoconversion rate given by the R_3 scheme is too large [*Baker*, 1993; *Austin et al.*, 1995; *Delobbe and Gallée*, 1998] suggest that the lower autoconversion rate in the R_6 scheme is more realistic. Recently, R. Wood (preprint, 2004, available at http://www.atmos.washington.edu/∼robwood/papers/drizpa1b.pdf) found that the R_6 scheme and the *Khairoutdinov and Kogan* [2000] scheme were much more accurate than the R_3 scheme, which strongly overestimated autoconversion. However, *Menon et al.* [2003] found that the R_3 scheme "severely underestimated" precipitation, so further work is needed to reconcile these differences.

[20] We also performed some sensitivity tests. First, we repeated the R6AUTO runs with the dispersion effect turned off in the autoconversion rate (i.e., we set β_6 = 1 in equation (2)). This test gave ΔCF = −0.22 W m^{-2}, a little smaller than the result from the R6AUTO run. This is consistent with the middle curve in Figure 2b having a slightly steeper average slope than the lowest curve. It further underlines that the absolute changes of P with N control the simulated second indirect effect, rather than the relative changes as described by the functional variation of P with N. Note that β_6 = 1 is the assumption that is usually made in the R_3 scheme, but it is equally valid to choose a larger value of β_6 to represent a droplet spectrum with fixed relative dispersion. A larger value of β_6 would give a larger autoconversion rate, and hence a larger second indirect effect. Next, we repeated R3AUTO and R6AUTO with N

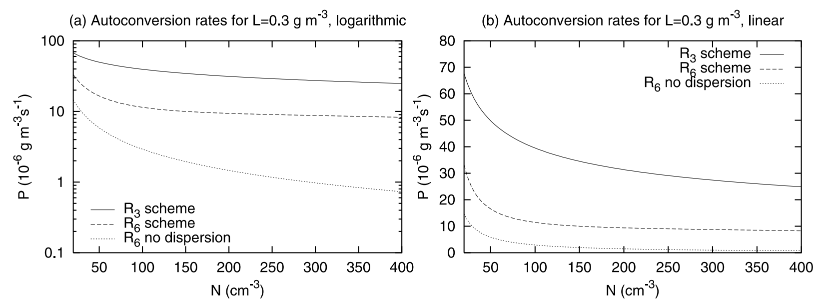

Figure 2. Autoconversion rates for L = 0.3 g m^{-3} given by the R_3 scheme, and by the R_6 scheme with and without the dispersion effect, using (a) logarithmic and (b) linear scales. See color version of this figure in the HTML.

allowed to vary in the radiation scheme as well as in the autoconversion scheme, to estimate the total indirect aerosol effect on liquid-water clouds. As above, the dispersion effect was included in the parameterization of effective radius [*Rotstayn and Liu*, 2003]. We obtained ΔCF = -1.63 W m^{-2} using the R_3 scheme, and -1.09 W m^{-2} using the R_6 scheme. The difference (0.54 W m^{-2}) is close to the difference between our estimates for the second indirect effect (0.43 W m^{-2}).

[21] The results obtained with the R_6 scheme are easier to reconcile with observations. For example, -1.09 W m^{-2} for the total indirect aerosol effect is much closer to the estimate of -0.85 W m^{-2} obtained when a GCM was constrained by satellite observations by *Lohmann and Lesins* [2002]. Also, the impact of the smaller autoconversion rate on the second indirect effect shows the importance of careful evaluation of autoconversion schemes and avoidance of artificial ''tuning'' of rates or thresholds.

[22] **Acknowledgments.** This work was funded in part by the Australian Greenhouse Office. Yangang Liu is supported by the US Department of Energy, as part of the Atmospheric Radiation Measurement Program, under contract DE-AC02-98CH10886.

References

Anderson, T. L., R. J. Charlson, S. E. Schwartz, R. Knutti, O. Boucher, H. Rodhe, and J. Heintzenberg (2003), Climate forcing by aerosols—A hazy picture, *Science*, *300*, 1103–1104.
Austin, P., Y. Wang, R. Pincus, and V. Kujala (1995), Precipitation in stratocumulus clouds: Observational and modeling results, *J. Atmos. Sci.*, *52*, 2329–2352.
Baker, M. B. (1993), Variability in concentrations of cloud condensation nuclei in the marine cloud-topped boundary layer, *Tellus, Ser. B*, *45*, 458–472.
Beard, K. V., and H. T. Ochs III (1993), Warm-rain initiation: An overview of microphysical mechanisms, *J. Appl. Meteorol.*, *32*, 608–625.
Boucher, O., H. Le Treut, and M. B. Baker (1995), Precipitation and radiation modelling in a GCM: Introduction of cloud microphysical processes, *J. Geophys. Res.*, *100*, 16,395–16,414.
Cooke, W. F., and J. J. N. Wilson (1996), A global black carbon aerosol model, *J. Geophys. Res.*, *101*, 19,395–19,409.
Delobbe, L., and H. Gallée (1998), Simulation of marine stratocumulus: Effect of precipitation parameterization and sensitivity to droplet number concentration, *Boundary Layer Meteorol.*, *89*, 75–107.
Ghan, S., et al. (2001), A physically based estimate of radiative forcing by anthropogenic sulfate aerosol, *J. Geophys. Res.*, *106*, 5279–5293.
Gordon, H. B., et al. (2002), The CSIRO Mk3 climate system model, *Tech. Pap. 60*, Atmos. Res., Commonw. Sci. and Ind. Res. Org., Aspendale, Victoria, Australia.
Han, Q., W. B. Rossow, J. Zeng, and R. Welch (2002), Three different behaviors of liquid water path of water clouds in aerosol-cloud interactions, *J. Atmos. Sci.*, *59*, 726–735.
Intergovernmental Panel on Climate Change (IPCC) (2001a), *Climate Change 2001: The Scientific Basis: Contribution of Working Group I to the Third Assessment Report of the Intergovernmental Panel on Climate Change (IPCC)*, edited by J. T. Houghton et al., Cambridge Univ. Press, New York.
Intergovernmental Panel on Climate Change (IPCC) (2001b), Aerosols, their direct and indirect effects, in *Climate Change 2001: The Scientific Basis: Contribution of Working Group I to the Third Assessment Report of the Intergovernmental Panel on Climate Change (IPCC)*, edited by J. T. Houghton et al., pp. 289–348, Cambridge Univ. Press, New York.
Jones, A., D. L. Roberts, M. J. Woodage, and C. E. Johnson (2001), Indirect sulphate aerosol forcing in a climate model with an interactive sulfur cycle, *J. Geophys. Res.*, *106*, 20,293–20,310.
Khairoutdinov, M., and Y. Kogan (2000), A new cloud physics parameterization in a large-eddy simulation model of marine stratocumulus, *Mon. Weather Rev.*, *128*, 229–243.
Kristjánsson, J. E. (2002), Studies of the aerosol indirect effect from sulfate and black carbon aerosols, *J. Geophys. Res.*, *107*(D15), 4246, doi:10.1029/2001JD000887.
Liu, Y. G., and P. H. Daum (2002), Indirect warming effect from dispersion forcing, *Nature*, *419*, 580–581.
Liu, Y., and P. H. Daum (2004), Parameterization of the autoconversion process. Part I: Analytical formulation of the Kessler-type parameterizations, *J. Atmos. Sci.*, *61*, 1539–1548.
Liu, Y., P. H. Daum, and R. McGraw (2004), An analytical expression for predicting the critical radius in the autoconversion parameterization, *Geophys. Res. Lett.*, *31*, L06121, doi:10.1029/2003GL019117.
Lohmann, U., and J. Feichter (2001), Can the direct and semi-direct aerosol effect compete with the indirect effect on a global scale?, *Geophys. Res. Lett.*, *28*, 159–161.
Lohmann, U., and G. Lesins (2002), Stronger constraints on the anthropogenic indirect aerosol effect, *Science*, *298*, 1012–1015.
Menon, S., A. D. Del Genio, D. Koch, and G. Tselioudis (2002), GCM simulations of the aerosol indirect effect: Sensitivity to cloud parameterization and aerosol burden, *J. Atmos. Sci.*, *59*, 692–713.
Menon, S., et al. (2003), Evaluating aerosol/cloud/radiation process parameterizations with single-column models and Second Aerosol Characterization Experiment (ACE-2) cloudy column observations, *J. Geophys. Res.*, *108*, 4762, doi:10.1029/2003JD003902.
O'Dowd, C. D., M. H. Smith, I. E. Consterdine, and J. A. Lowe (1997), Marine aerosol, sea-salt, and the marine sulphur cycle: A short review, *Atmos. Environ.*, *31*, 73–80.
Peng, Y., and U. Lohmann (2003), Sensitivity study of the spectral dispersion of the cloud droplet size distribution on the indirect aerosol effect, *Geophys. Res. Lett.*, *30*(10), 1507, doi:10.1029/2003GL017192.
Rotstayn, L. D. (1997), A physically based scheme for the treatment of stratiform clouds and precipitation in large-scale models: I. Description and evaluation of the microphysical processes, *Q. J. R. Meteorol. Soc.*, *123*, 1227–1282.
Rotstayn, L. D. (2000), On the ''tuning'' of autoconversion parameterizations in climate models, *J. Geophys. Res.*, *105*, 15,495–15,507.
Rotstayn, L. D., and Y. Liu (2003), Sensitivity of the first indirect aerosol effect to an increase of cloud droplet spectral dispersion with droplet number concentration, *J. Clim.*, *16*, 3476–3481.
Rotstayn, L. D., and U. Lohmann (2002), Simulation of the tropospheric sulfur cycle in a global model with a physically based cloud scheme, *J. Geophys. Res.*, *107*(D21), 4592, doi:10.1029/2002JD002128.
Suzuki, K., T. Nakajima, A. Numaguti, T. Takemura, K. Kawamoto, and A. Higurashi (2004), A study of the aerosol effect on a cloud field with simultaneous use of GCM modeling and satellite observation, *J. Atmos. Sci.*, *61*, 179–194.

Y. Liu, Atmospheric Sciences Division, Brookhaven National Laboratory, Bldg. 815E, 75 Rutherford Dr., Upton, NY 11973, USA. (lyg@bnl.gov)
L. D. Rotstayn, Atmospheric Research, CSIRO, PB1, Aspendale, Vic, 3195, Australia. (leon.rotstayn@csiro.au)